مجلة كلية التربية الاساسية
كلية التربية الاساسية – الجامعة المستنصرية
Journal of the College of Basic Education Vol.30 (NO. 125) 2024, pp. 53-73

Biosynthesis and Structural Properties of Sulfur Nanoparticles Using *Proteus mirabilis* Extract and its Effect on Pathogenic Bacteria

[1]Arkan J. Nima
[2]Suzan Saadi Hussain
[3]Nawfal H. Aldujaili

[1] *Department of Biology, College of Science, Mustansiriyah University, Baghdad, Iraq.*
[2] *Department of Biology, College of Science, Mustansiriyah University, Baghdad, Iraq.*
[3] *Department of Biology, Faculty of Science, University of Kufa, Alnajaf, Iraq*
Corresponding authors:
[1] *arkanjabbar.ms.c.mic.2020@uomustansiriyah.edu.iq*
[2] *suzansaadialroznamachi@uomustansiriyah.edu.iq*
[3] *nawfal.aldujaili@uokufa.edu.iq*

Abstract:

This research focuses on exploring the therapeutic potential of sulfur nanoparticles (sulfur NPs) synthesized from *Proteus mirabilis* (*P. mirabilis*) extract against *Staphylococcus aureus* (*S. aureus*), a pathogen implicated in skin infections. The study identified significant inhibitory effects of these nanoparticles on biofilm-producing and multidrug-resistant *S. aureus* isolates (A5, A8, A9, A11, and A29), with minimum inhibitory concentrations ranging from 16 to 32 µg/mL. While the study found no statistically significant differences in inhibition rates across various nanoparticle concentrations ($p=0.842$), there was a notable increase in anti-biofilm activity with higher concentrations ($p<0.05$). For instance, at 1024 µg/mL, the inhibition rate was approximately 93.1%, compared to 5.2% at 2 µg/mL ($p=0.0001$). These findings underscore the promising antimicrobial efficacy of sulfur NPs derived from *P. mirabilis* in combating drug-resistant *S. aureus* infections and biofilm formation commonly associated with dermatitis.

Keywords:, *Staphylococcus aureus* ,sulfur nanoparticles, antimicrobial, antibiofilm, *Proteus mirabilis*.

1.Introduction

S. aureus species are the most opportunistic pathogenic bacterial species, can cause various infections in patients with immune compromised or immune competent.The Nasal cavity of human is the major habitat for this species, but it also presents in the oral cavity, on the skin, inside skin glands,and in the gastrointestinal tract (Cheung GYC 2021, 12). Antibiotic resistance in *S. aureus* isolates is a common occurrence, making *S. aureus* infections particularly troublesome. Methicillin-resistant *S. aureus* (MRSA) is the most significant clinically (Idrees M 2021, 18; Hussain SS 2017, 10).

Unlike several other bacterial pathogens, which frequently depend on just one or a few toxins to cause illness, *S. aureus* generates an incredible variety of virulence factors. These comprise a wide range of protein and non-protein components that facilitate host colonisation during infection, as well as an abundance of poisons and immune evasion mechanisms. Since *S. aureus* was identified as a significant pathogen at the end of the 19th century, there has always been a great deal of interest in its virulence. However, recent advancements have prompted further research into the processes behind *S. aureus* virulence (Cheung GYC 2021, 12).

Nanoparticle-based therapeutic treatment has emerged as a promising alternative strategy for combating *S. aureus* and its biofilm. Studies have shown that sulfur NPs possess significant bioactivity against various pathogenic bacteria, including *S. aureus* (Kim YH 2020, 144). Apart from their antimicrobial properties, these nanoparticles exhibit a wide range of biological activities, including anticancer and antioxidant effects. Furthermore, these sulfur nanoparticles can eliminate harmful reactive oxygen species (ROS) (Priyadarshi R 2022, 20).

Bacterial biofilms are embedded in an extracellular matrix employing distinct gene expression patterns. Chronic infections with a complicated resistance to both immune defences and antibiotics are caused by biofilms. As a result, biofilm infections present more difficult removal problems
(Ali AM, Abdallah 2022, 33).

Various techniques have been employed for the production of sulfur NPs thus far. However, these methods have limitations, such as being energy-intensive and involving complex, time-consuming, and potentially hazardous procedures. To overcome or mitigate these challenges, there is a need for

advancements in nanotechnology to enhance existing synthetic approaches. Nanoparticle biosynthesis can take place either intracellularly or extracellularly. However, extracellular methods are generally preferred because intracellular biosynthesis requires additional steps, such as cell lysis, extraction, and purification of the produced nanoparticles (Mahdi SA 2021, 52). Pathogenic bacteria, including *P. mirabilis*, can biosynthesize nanoparticles in vitro. No previous studies have reported the biosynthesis of sulfur NPs by *P. mirabilis*. Consequently, this study represents the first report demonstrating the ability of *P. mirabilis* to produce sulfur NPs under the aforementioned conditions. Although specific information regarding the interaction of *P. mirabilis* with sulfur compounds and nanoparticle formation is lacking, several studies have identified *P. mirabilis* as a proficient producer of nanoparticles. For instance, Karthick and their teammates successfully biosynthesized silver nanoparticles using *P.mirabilis* (Karthick K 2013, 5), while Wang and their teammates demonstrated the bacterium's capacity to produce selenium nanoparticles (Wang Y 2018, 19).

Thus, the recent work aimed to investigate the process of synthesizing sulfur NPs using the bacterium *P. mirabilis* and understanding their structural properties, in addition to evaluation of its potential antimicrobial effects on pathogenic bacteria, *S. aureus.*

2.Materials and Methods

2.1. Bacterial isolates

The five isolates of multi-drug resistant, biofilm-producing *S. aureus* were obtained from patients with skin infections at Yarmouk Teaching Hospital and Al-Kindi Teaching Hospital. Additionally, a single isolate of *P. mirabilis* was identified using different examinations.

2.2. Biosynthesis of sulfur NPs using *P. mirabilis*

To prepare a supernatant of *P. mirabilis*, a nutritional broth medium was used. An orbital shaker was used to incubate the culture flasks at 37 degrees Celsius while they were stirred at 220rpm. After 24hrs of growth, the biomass was collected and centrifuged at a speed of 10000 rpm for 15min. The material that was taken from the supernatant was going to be used in the subsequent process that would produce Sulfur NPs (Karthick K 2013, 5; Jubran AS 2020, 11).

Following the references (Al Banna LS 2020, 6; Khairan K, Jalil Z 2019, 12), the preparation process was conducted as follows: 250 ml of deionized water were mixed with 10 g of sodium thiosulfate ($Na_2S_2O_3.5H_2O$) using a magnetic stirrer for one hour. Then, 40 ml of freshly prepared *P. mirabilis* bacterial solution was added to the mixture and stirred for an additional two hours. To facilitate the production of sulfur NPs, hydrochloric acid (12 ml / 300 ml of deionized water) was added after achieving full homogeneity. The precipitate was subsequently washed with ethanol and distilled water before being separated by centrifugation. Finally, the sample was heated at 50°C for and dried in a hot air oven.

2.3. Characterization of biosynthesized sulfur NPs

Various technologies were employed to characterize sulfur NPs including UV-visible spectroscopy analysis, field emission scanning electron microscope (FE-SEM) analysis, energy dispersive X-ray spectroscopy (EDS) analysis, X-ray diffraction (XRD) analysis, transmission electron microscopy (TEM) analysis, and Fourier Transform Infrared (FTIR) analysis.

2.4. Antibacterial activities of sulfur NPs.

The antibacterial effects of sulfur NPs were investigated using the agar well diffusion method against multidrug-resistant (MDR) bacteria and biofilm-forming *S. aureus* isolates obtained from skin infections. Five fresh colonies of *S. aureus* were suspended in 5 milliliters of Brain Heart Infusion Broth (BHIB) and incubated for 18 hours at 37°C. To achieve an optical density corresponding to the 0.5 McFarland criteria (1.5 x 108 cells/ml), the turbidity of the grown culture was adjusted using sterilized broth. The suspensions were then applied to sterile cotton swabs and used to streak the entire surface of Mueller Hinton Agar trays. Three wells were made in each dish using a sterile cork, and each well was filled with 150 µl of sulfur NPs at three different concentrations (100, 200, and 300 µg/ml). The Petri dishes were incubated at 37°C for 24 hours. The diameter of the growth inhibition zones, measured in millimeters, was used to assess the antibacterial effect (Vahdati M, Tohidi M 2020, 10).

2.5 Minimum Inhibitory Concentration (MIC) analysis of sulfur NPs.

The minimum inhibitory concentrations (MIC) of sulfur NPs were determined using the microtiter plate method. Serial dilutions of sulfur NPs (1024, 512, 256, 128, 64, 32, 16, 8, 4, and 2 µg/ml) were prepared using 100 µl of Mueller Hinton broth as the diluent. The microtiter plate wells were set up as follows: the negative control wells contained 200 µl of Mueller Hinton broth only, the positive control wells contained Mueller Hinton broth and 10 µl of bacterial suspension without sulfur NPs, and in well(2) contained 100 µl of a high concentration of nano-sulfur was withdrawn and added. All wells from 2 to 11 received a 10 µl bacterial suspension of *S. aureus* corresponding to the McFarland standard no. 0.5 (1.5 x 108 CFU/ml). The microtiter plates were then incubated at 37°C for 18 to 20 hours. To detect color changes, 30 µl of Resazurin dye was added to each well and incubated for two hours. The MIC of the sulfur NPs was determined based on the color shift from blue to pink in the Resazurin dye broth experiment. The sub-MIC values were visually assessed by observing any color changes in the broth microdilutions (Ohikhena FU 2017, 2017).

2.6 Anti-biofilm effect by sulfur NPs.

The in vitro antibiofilm activity was assessed using the 96-well microtiter plate method. The first well of the microtiter plate was filled with 100 µL of BHIB medium containing 1% sucrose and 100 µL of biosynthesized sulfur NPs. Dilutions of the sulfur NPs were prepared at various concentrations (1024, 512, 256, 128, 64, 32, 16, 8, 4, and 2 µg/ml). To assess the growth of biofilm by bacteria and the inhibitory effect of sulfur NPs on biofilm formation, 100 µL of the diluted concentration was added to each well of the microtiter plate, with the last well serving as a control. Then, 10 µL of overnight-cultivated isolated *S. aureus* bacteria were added to each well. The microtiter plates were incubated at 37 °C for 24 hours. To remove free-floating "planktonic" bacteria, the contents of each well were aspirated and washed three times with 0.2 mL of phosphate-buffered saline (PBS, pH 7.2). The biofilms formed by adherent bacteria on the walls of the plate were fixed with 2% w/v sodium acetate and stained with 0.1% w/v crystal violet dye. Excess stain was washed off with sterile deionized water, and the plates were allowed to dry. After drying, 200 µL of 95% v/v ethanol were added to the wells (Shakibaie M 2019, 6). The optical densities (OD) were measured using

an ELISA reader set at 570 nm to assess bacterial attachment to the wells and biofilm formation. The measurements were performed three times to ensure accuracy and consistency. The OD values indicated the extent of biofilm formation. To calculate the percentage of bacterial biofilm inhibition by sulfur NPs concentration, the following equation incorporating the OD values was utilized (Barapatre A 2016, 3):

% biofilm inhibition =

$$[1 - (OD\ of\ cells\ treated\ with\ SNPs\ /OD\ of\ non - treated\ control)\ x\ 100]$$

3. Results and Discussion

3.1. Biosynthesis of sulfur NPs using extract of *P. mirabilis*

The extract for *P. mirabilis* which was employed in the biosynthesis of sulfur NPs, displayed extracellular biosynthesis after adding extract to sodium thiosulfate as a base material under previously adjusted conditions, including pH 7 and extract concentration, utilizing cell free supernatant for extract. The color shift of the reaction mixture into yellowish white.

There was no study reported to biosynthesize sulfur NPs by pathogenic bacterial species. Hence, this study was the first study reported that pathogenic *P. mirabilis* extract was showed its ability to produce sulfur NPs under previously mentioned conditions. In terms of interaction with sulfur compounds and nanoparticle formation, there isn't specific information available about *P. mirabilis* producing sulfur NPs. However, *P. mirabilis* extract has been identified as good nanoparticles' producer in several studies. (Karthick K 2013, 5) reported biosynthesis of silver nanoparticles were prepared from *P.mirabilis* extract, whereas this bacterium also show its potential to produce Selenium nanoparticle, as conducted by (Wang Y 2018, 19).

3.2. Characterization of sulfur NPs

3.2.1. UV–visible spectroscopy analysis

UV–vis spectroscopy is a crucial technique to ascertain the stability and formation of sulfur NPs. Figure (1) showed that the peak of sulfur NPs at 200nm, which indicating the successful formation of sulfur NPs (Paralikar P, Rai M 2018, 12).

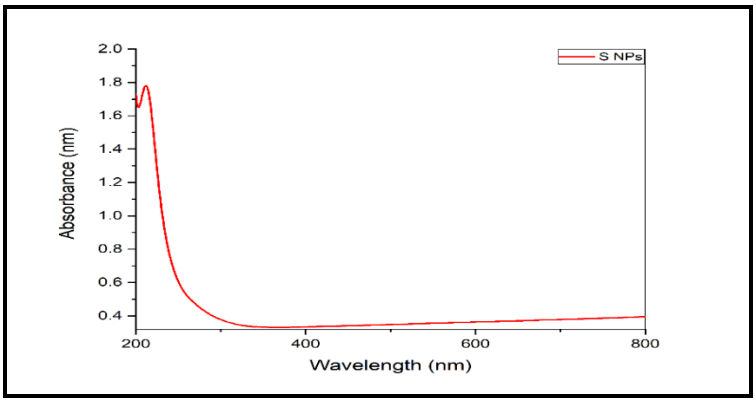

Figure (1): UV-visible spectra of sulfur NPs.

3.2.2. Transmission electron microscopy (TEM) analysis

Figures (2,A) showed the TEM image of sulfur NPs, whereas it is noticeable

that the shape of the nanoparticles is spherical or semi-spherical, with the size less than 100 nm. This again confirms the formation of the particles in nanoscale. There are some particles tended to agglomerate, where have size slightly larger than 100 nm, this may be due to the presence of the protein that surrounds the nanoparticles. Form both SEM and TEM figures; we can say sulfur has a tends agglomeration (Suleiman M 2015, 6).

3.2.3 Field Emission Scanning Electron Microscope (FE-SEM) analysis

The FE-SEM images of the sulfur NPs represented in Figure (2,B). The images indicate that nanoparticles prepared via suggested method are almost spherical in shape and uniform size with an average diameter almost 30.70 nm. The sulfur crystals agglomerate, creating an irregular appearance of nanoparticles.

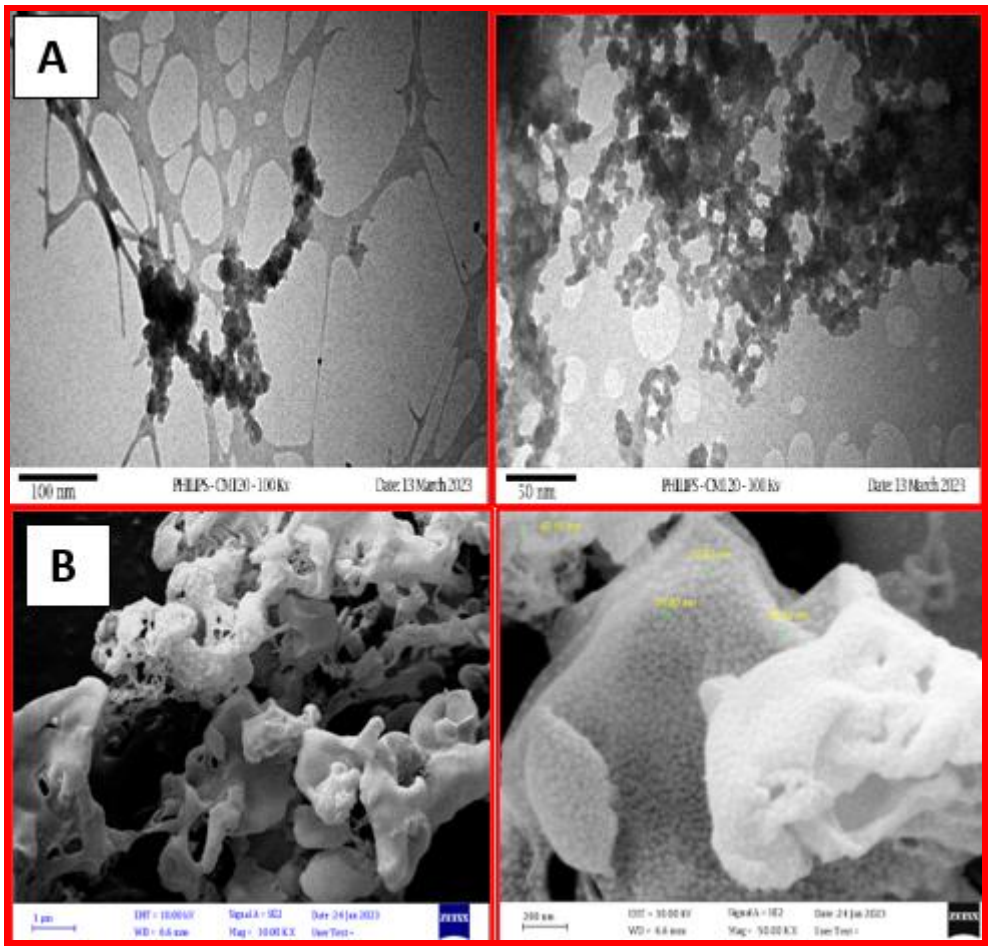

Figure (2): A) TEM images and B) FE-SEM of sulfur NPs synthesized by *Proteus mirabilis* extract

3.2.4. Energy Dispersive (EDS) X-Ray spectroscopy analysis

Energy Dispersive Spectroscopy was used to quantify the presence of NPs by observing the optical absorption peaks of elements. Elemental analysis exhibited the percentage of elements constituent of sulfur and Oxygen as shown in insert figure (3, A). In addition, the appearance of Au element is to the supports used on the substrate during the measurement. The results confirm the formation of sulfur and there are no other impurities.

3.2.5 X-ray diffraction (XRD) analysis

Figure (3, B) display XRD diffraction of sulfur NPs that prepared by *P. mirabilis* extract. It observed presence the main peaks of sulfur according to

standard sulfur particle diffraction pattern (JCPD). Table (1) summary of results XRD diffraction (Suleiman M 2015, 6).

3.2.6 Fourier Transform Infrared analysis (FTIR)

Figure (3,C) shows the FTIR spectra which display strong absorption bands at 3435 cm^{-1} could be ascribed to the stretching absorption band hydroxyl (–OH) stretching H-bonded phenols. The peaks at 2925 and 2854 cm-1 could be assigned to the asymmetric and symmetric stretching of–CH_2 and -CH_3 functional groups of aliphatic. The peak at 1642 cm-1 is characteristic of amide carbonyl group in amide I and amide II. C-N stretch of aromatic amines and carboxylic acids gives rise to band at 1379 cm-1. The peak at 1118 cm-1 is due to the vibration mode of C-O. 647 cm-1 can be assigned to bending modes of aromatic and weak peak at 471 due to bond sulfur NPs (Salem NM 2016, 8).

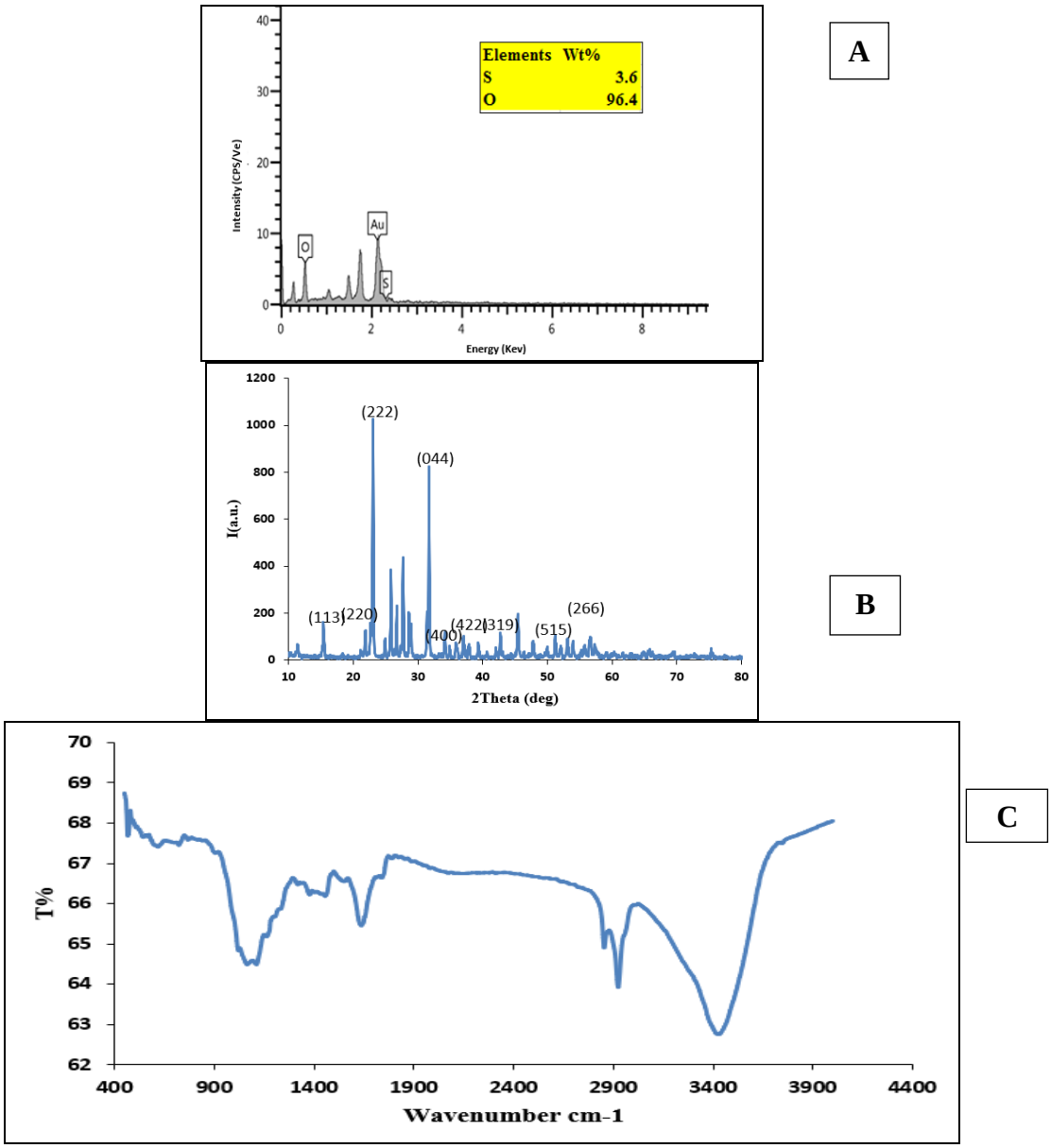

Figure (3): A) EDS, B) XRD and C) FTIR of sulfur NPs synthesized by *P. mirabilis* extract.

Table (1) summary of results XRD diffraction .

Sample	2Theta (deg)	D (A)	FWHM (deg)	C.S (nm)	Hkl
sulfur nanoparticles	15.74	5.73	0.15	53.60	113
	22.14	3.91	0.15	54.10	220
	23.39	3.84	0.14	57.43	222
	31.74	2.84	0.16	51.74	044
	34.54	2.62	0.14	59.56	400
	37.39	2.42	0.20	42.03	422
	42.84	2.14	0.18	47.51	319
	47.99	1.90	0.24	36.30	515
	51.46	1.75	0.16	55.2	266

3.3 Antibacterial Activity of sulfur NPs

The study showed that sulfur NPs synthesized by extract of *P. mirabilis* has an inhibitory growth effect against five biofilm producers and MDR bacterial isolates of *S. aureus* (A5, A8, A9, A11 and A29). The agar well diffusion method was primary method which used for detecting the antibacterial activity of sulfur NPs with different concentrations (100, 200 and 300 µg/ml). sulfur NPs exhibited antimicrobial activity against examined bacteria with inhibition zone ranged between 14 to 18, 15 to 20 and 18 to 25 mm at 100, 200 and 300 µg/ml, respectively. The largest inhibition zone of sulfur NPs was (25 mm) against *S. aureus* A5 by a concentration of 300 µg/ml, whereas the lowest inhibition zone was (14 mm) against *S. aureus* A8, A9 and A11 at the concentration of 100 µg/ml, as shown in figure (4:A,B).

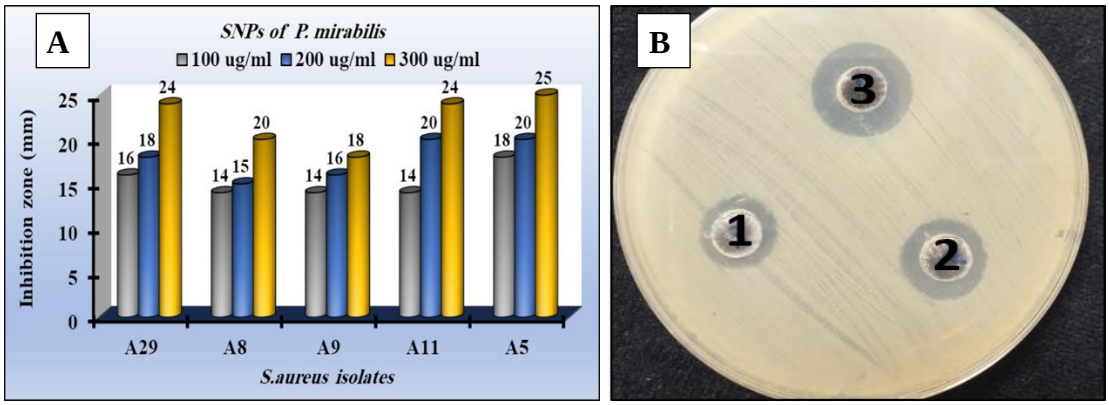

Figure (4):A) The antimicrobial activity of sulfur NPs biosynthesized by *P. mirabilis* extract against five isolate of *S. aureus* .B) Isolate (A9) in Mueller-Hinton agar under concentration of (1: 100 µg/ml; 2: 200 µg/ml; 3: 300 µg/ml).

The antimicrobial activities of sulfur NPs synthesized using the aforementioned extracts were found to be dependent on their concentration. The effectiveness of sulfur NPs increased as their concentration increased, consistent with the findings of (Niranjan R 2022, 12).The assessment of antimicrobial activity of sulfur NPs is influenced by critical factors. For instance, the rate of diffusion and bioavailability of nanoparticles in different media, such as broth and agar, may vary for different organisms, as highlighted by (Suleiman M 2015, 6). The scientific community is striving to develop successful alternatives to current antibiotics that are facing resistance issues, as well as effective new drugs to complement antibiotics, given the growing problem of multidrug resistance (MDR). Nanoparticles are being explored as a potential alternative to antibiotics, with the potential to address the issue of bacterial MDR (Morone et al., 2022). The findings of this study are in agreement with those of (Paralikar P, Rai M 2018, 12), who reported a continuous decrease in the slope of bacterial growth curves with increasing nanoparticle concentration (50, 100, 150, and 200 µg/ml). They observed that sulfur NPs started inhibiting the growth of *E. coli* and *S. aureus* at concentrations around 150-200 µg/ml. At a concentration of 200 µg/ml, sulfur NPs exhibited bactericidal activity against both test organisms. It was also noted that in the absence of sulfur NPs, the optical density (OD) increased, indicating an increase in bacterial growth. This suggests that at

lower concentrations of sulfur NPs, bacterial growth was delayed, while at higher concentrations, growth was completely inhibited. In a study conducted by Saedi et al. (Saedi S 2020, 13), sulfur NPs demonstrated good antimicrobial activity against *S. aureus*, with inhibition zone sizes ranging between 13.0 to 14.7 mm. Suleiman et al. reported significant antibacterial activity of sulfur NPs (5.47 µg/ml) against Gram-positive bacteria (*S. aureus)* with 5.7 nm, but no activity against Gram-negative bacteria (*E. coli* and *P. aeruginosa*), even at a high concentration of 800 µg/ml . They explained that the outer membrane of Gram-negative bacteria provides protection, acting as a barrier that restricts or prevents the penetration of sulfur NPs into bacterial cells and may promote self-aggregation between nanoparticles (Suleiman M 2015, 6). The antimicrobial properties of several metal nanoparticles have been extensively studied, including their mechanisms of action. Possible mechanisms may involve the strong interaction of sulfur NPs (which are negatively charged) with target molecules such as enzymes and proteins on the cell surface, leading to the formation of pits and leakage of cellular components. It is also hypothesized that sulfur NPs, like silver nanoparticles, generate sulfur ions that subsequently form toxic H2S, which interacts with -SH groups, induces oxidative stress, and denatures proteins and lipids. Another possibility is the formation of H2S through the reduction of sulfur NPs by unknown molecules like NADH. Additionally, there is a potential for sulfur NPs to interact with DNA, leading to its destruction and cell death (Rai M 2016, 14).

3.4 Determination of minimum inhibitory concentration of sulfur NPs

Different concentrations, including 1024, 512, 256, 128, 64, 32, 16, 8, 4 and 2 µg/mL, of sulfur NPs, were utilized in this step. The results illustrated that the MIC of sulfur NPs was 16 µg/mL of isolates of *S. aureus* A5, A8 and A29, while their sub-MIC was 8 µg/mL. Also, the MIC of sulfur NPs was 32 µg/mL for isolates of *S. aureus* A9 and A11, while their sub-MIC was 16 µg/mL, as shown in table (2) and figure (5).

Table (2): The results of MIC and sub-MIC of sulfur NPs.

S.NPs extract	*S. aureus* Isolates	S. NPs MIC (µg/mL)	S. NPs Sub-MIC (µg/mL)
P. mirabilis	A5	16	8
	A8	16	8
	A9	32	16
	A11	32	16
	A29	16	8

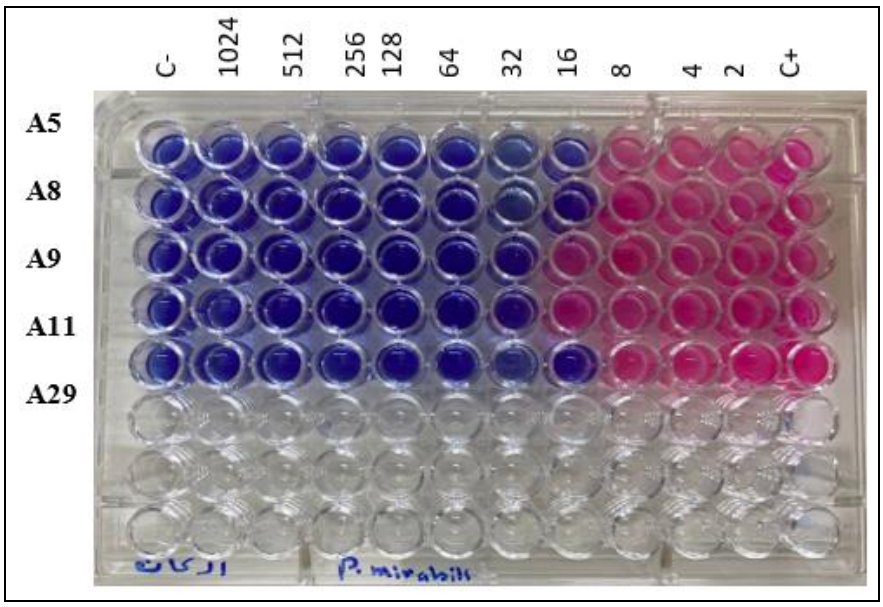

Figure (5): Determination of MIC and sub-MIC of sulfur NPs biosynthesized using bacterial extract of *P. mirabilis*.

3.5. Anti-Biofilm Activity of sulfur NPs

Only five strong-biofilm producers and MDR bacterial isolates of *S. aureus* (A5, A8, A9, A11 and A29) were used to assess the ability of sulfur NPs as anti-biofilm agent to inhibit biofilm. Relying on previous research (Babapour E 2016, 6; Sultan AM, Nabiel Y, 2019, 20) was calculate the biofilm formation and biofilm development was categorized as strong, moderate, or non/weak. The results of statistical analysis in the table (3) show no significant differences ($p>0.05$) in inhibition rate of all strain isolates (A5, A8, A9, A11 and A29) for all concentrations of sulfur NPs with $p=0.842$.

Furthermore, the effects of different concentrations of sulfur NPs indicated that same isolates to significant ($p<0.05$) increase in inhibition rate (activity as antibiofilm) proportional with elevated of sulfur NPs concentrations, whereas was the mean± SE inhibition rate at 1024 ug/ml from *P. mirabilis* was about 93.1±0.8 %, when compared with decreased sulfur NPs concentrations at 2 ug/ml, which was about 5.2±1.2 %, with p=0.0001, respectively. The antibiofilm effectiveness results differ depending on the bacterial strains.

Table (3): Anti-biofilm activity of sulfur NPs against *S. aureus* isolates.

S.NPs synthesis	**Concentration**	**Inhibition % (killing rate %)**						***p*-value [#]**
		A29	**A8**	**A5**	**A11**	**A9**	**Mean ± SE**	
Sulfur NPs of *P. mirabilis*	**1024**	93.8	92.0	95.0	94.3	90.5	93.1±0.8	**0.842 ns**
	512	91.5	89.6	82.1	83.6	85.1	86.4±1.8	
	256	84.0	80.5	76.0	74.3	76.2	78.2±1.8	
	128	72.3	70.8	70.9	65.5	46.4	65.2±4.8	
	64	69.4	67.1	69.2	35.2	32.9	54.8±8.5	
	32	34.3	66.2	37.6	32.3	18.5	37.8±7.8	
	16	30.9	37.4	34.6	24.0	13.3	28.0±4.3	
	8	20.3	19.9	23.6	13.9	10.9	17.7±2.3	
	4	8.9	13.7	11.3	4.0	5.4	8.6±1.8	
	2	5.9	8.3	7.3	2.8	2.0	5.2±1.2	
p-value [¥]		**0.0001***						

Biofilms provide an advantageous environment for bacteria, offering protection against the host's immune system, displaying resistance to antimicrobial agents, and facilitating resource distribution within the

microbial population. These characteristics make biofilm bacteria more challenging to treat compared to planktonic cells (Fulaz S 2019, 27). Sulfur NPs have demonstrated inhibitory effects on the formation of biofilms by *S. aureus*, a bacterium commonly associated with various human infections. The unique properties of sulfur NPs, including their small size, large surface area, and chemical reactivity, contribute to their effectiveness in inhibiting biofilm formation (Lahiri D 2021, 12). Studies have shown that sulfur NPs can inhibit *S. aureus* biofilm formation over a 48-hour period, while they do not exhibit inhibitory effects on *P. aeruginosa* biofilm formation (Dop RA 2023, 15). The interactions between nanoparticles and biofilms can be described through three sequential mechanisms: the transport of NPs to the biofilm-fluid interface, attachment to the outer region of the biofilm surface, and migration within the biofilm (Ikuma K 2015, 15). The physicochemical properties of NPs, such as size, shape, surface charge, hydrophobicity, and functional groups, influence their interaction with biofilm components, both in the extracellular polymeric substance (EPS) matrix and on the bacterial surface (Canesi L, Corsi I 2016, 565). Generally, positively charged NPs are more likely to interact with EPS substances, which, as a whole, carry a negative charge (Huangfu X 2019, 219). NPs can alter gene expression related to biofilm formation, thereby affecting microcolony formation and biofilm maturation. This suggests that NPs could be utilized for preventing and treating biofilm-related infections (Hasan A 2018, 563). Hydroxyl radicals generated by NPs can depolymerize polysaccharides, cause DNA breaks, and inactivate enzymes, thereby compromising the EPS matrix and biofilm architecture (Applerot G 2012, 8).

The result confirm the promising antimicrobial properties of sulfur NPs derived from *P.mirabilis* extract against multidrug-resistant, biofilm-forming *S.aureus* associated with dermatitis. Further research is warranted to clarify its safety profile and long-term efficacy for clinical applications. This study opens avenues for exploring natural sources for innovative antimicrobial solutions in combating antibiotic resistance. The use of *P.mirabilis* extract for the synthesis of Sulfur NPs not only represents a major advance in the development of antimicrobial nanoparticles, but also opens new ways to harness other bacterial extracts in the synthesis of Sulfur NPs. Moreover, the

use of bacterial extracts for synthesis sulfur NPs holds promise for cost-effective nanoparticle manufacturing. Compared to conventional chemical synthesis methods.

4.References

1. Cheung GYC, Bae JS, Otto M. Pathogenicity and virulence of Staphylococcus aureus. *Virulence*. 2021;12(1):547-569.
2. Hussain SS. Antibiofilm and Antibacterial Activity of Sodium Deoxycholate on *P. aeruginosa* and *Staph. aureus*. Journal of University of Babylon for Pure and Applied Sciences. 2017 10;25(5):1906-16.
3. Idrees M, Sawant S, Karodia N, Rahman A. Staphylococcus aureus biofilm: Morphology, genetics, pathogenesis and treatment strategies. *Int J Environ Res Public Health*. 2021;18(14):7602.
4. Kim YH, Kim GH, Yoon KS, Shankar S, Rhim JW. Comparative antibacterial and antifungal activities of sulfur nanoparticles capped with chitosan. *Microb Pathog*. 2020;144:104178.
5. Priyadarshi R, Riahi Z, Rhim JW, Kim JT. Comparison of physicochemical and functional properties of elemental sulfur, sulfur nanoparticles, and sulfur quantum dots for sustainable biological applications. *Materials Today Sustainability*. 2022;20:100243.
6. Ali AM, Abdallah MM. Study of Phenotypic and Genotypic Factors of Staphylococcus aureus Clinical Local Isolates. *Al-Mustansiriyah Journal of Science*. 2022;33(4):49-56.
7. Mahdi SA, Kadhim AA, Albukhaty S, et al. Gene expression and apoptosis response in hepatocellular carcinoma cells induced by biocompatible polymer/magnetic nanoparticles containing 5-fluorouracil. *Electronic Journal of Biotechnology*. 2021;52:21-29.
8. Karthick K, Kumaravel P, Hemalatha P, Thamaraiselvi L. Mechanistic aspects: Biosynthesis of Silver nanoparticles from Proteus mirabilis and its antimicrobial study. *Research Journal of Science and Technology*. 2013;5(2):235-238.

9. Wang Y, Shu X, Hou J, et al. Selenium nanoparticle synthesized by Proteus mirabilis YC801: an efficacious pathway for selenite biotransformation and detoxification. *Int J Mol Sci*. 2018;19(12):3809.
10. Jubran AS, Al-Zamely OM, Al-Ammar MH. A study of iron oxide nanoparticles synthesis by using bacteria. *Int J Pharm Qual Assur*. 2020;11(01):1-8.
11. Khairan K, Jalil Z. GREEN SYNTHESIS OF SULPHUR NANOPARTICLES USING AQUEOUS GARLIC EXTRACT (Allium sativum). *Rasayan Journal of Chemistry*. 2019;12(1).
12. Al Banna LS, Salem NM, Jaleel GA, Awwad AM. Green synthesis of sulfur nanoparticles using Rosmarinus officinalis leaves extract and nematicidal activity against Meloidogyne javanica. *Chemistry International*. 2020;6(3):137-143.
13. Vahdati M, Tohidi Moghadam T. Synthesis and characterization of selenium nanoparticles-lysozyme nanohybrid system with synergistic antibacterial properties. *Sci Rep*. 2020;10(1):510.
14. Ohikhena FU, Wintola OA, Afolayan AJ. Evaluation of the antibacterial and antifungal properties of Phragmanthera capitata (Sprengel) Balle (Loranthaceae), a mistletoe growing on rubber tree, using the dilution techniques. *The Scientific World Journal*. 2017;2017.
15. Shakibaie M, Alipour-Esmaeili-Anari F, Adeli-Sardou M, et al. Antibacterial and anti-biofilm effects of microwave-assisted biologically synthesized zinc nanoparticles. *Nanomed J*. 2019;6(3).
16. Barapatre A, Aadil KR, Jha H. Synergistic antibacterial and antibiofilm activity of silver nanoparticles biosynthesized by lignin-degrading fungus. *Bioresour Bioprocess*. 2016;3:1-13.
17. Paralikar P, Rai M. Bio-inspired synthesis of sulphur nanoparticles using leaf extract of four medicinal plants with special reference to their antibacterial activity. *IET Nanobiotechnol*. 2018;12(1):25-31.

18. Suleiman M, Al-Masri M, Al Ali A, et al. Synthesis of nano-sized sulfur nanoparticles and their antibacterial activities. *J Mater Environ Sci*. 2015;6(2):513-518.
19. Salem NM, Albanna LS, Abdeen AO, Ibrahim QI, Awwad AM. Sulfur nanoparticles improves root and shoot growth of tomato. *J Agric Sci*. 2016;8(4):179.
20. Niranjan R, Zafar S, Lochab B, Priyadarshini R. Synthesis and characterization of sulfur and sulfur-selenium nanoparticles loaded on reduced graphene oxide and their antibacterial activity against gram-positive pathogens. *Nanomaterials*. 2022;12(2):191.
21. Morone MV, Dell'Annunziata F, Giugliano R, et al. Pulsed laser ablation of magnetic nanoparticles as a novel antibacterial strategy against gram positive bacteria. *Applied Surface Science Advances*. 2022;7:100213.
22. Saedi S, Shokri M, Rhim JW. Antimicrobial activity of sulfur nanoparticles: effect of preparation methods. *Arabian Journal of Chemistry*. 2020;13(8):6580-6588.
23. Rai M, Ingle AP, Paralikar P. Sulfur and sulfur nanoparticles as potential antimicrobials: from traditional medicine to nanomedicine. *Expert Rev Anti Infect Ther*. 2016;14(10):969-978.
24. Babapour E, Haddadi A, Mirnejad R, Angaji SA, Amirmozafari N. Biofilm formation in clinical isolates of nosocomial Acinetobacter baumannii and its relationship with multidrug resistance. *Asian Pac J Trop Biomed*. 2016;6(6):528-533.
25. Sultan AM, Nabiel Y. Tube method and Congo red agar versus tissue culture plate method for detection of biofilm production by uropathogens isolated from midstream urine: Which one could be better? *African Journal of Clinical and Experimental Microbiology*. 2019;20(1):60-66.
26. Fulaz S, Vitale S, Quinn L, Casey E. Nanoparticle–biofilm interactions: the role of the EPS matrix. *Trends Microbiol*. 2019;27(11):915-926.

27. Lahiri D, Nag M, Sheikh HI, et al. Microbiologically-synthesized nanoparticles and their role in silencing the biofilm signaling cascade. *Front Microbiol*. 2021;12:636588.
28. Dop RA, Neill DR, Hasell T. Sulfur-Polymer Nanoparticles: Preparation and Antibacterial Activity. *ACS Appl Mater Interfaces*. 2023;15(17):20822-20832.
29. Ikuma K, Decho AW, Lau BLT. When nanoparticles meet biofilms—interactions guiding the environmental fate and accumulation of nanoparticles. *Front Microbiol*. 2015;6:591.
30. Canesi L, Corsi I. Effects of nanomaterials on marine invertebrates. *Science of the total environment*. 2016;565:933-940.
31. Huangfu X, Xu Y, Liu C, et al. A review on the interactions between engineered nanoparticles with extracellular and intracellular polymeric substances from wastewater treatment aggregates. *Chemosphere*. 2019;219:766-783.
32. Hasan A, Morshed M, Memic A, Hassan S, Webster TJ, Marei HES. Nanoparticles in tissue engineering: Applications, challenges and prospects. *Int J Nanomedicine*. Published online 2018:5637-5655.
33. Applerot G, Lellouche J, Lipovsky A, et al. Understanding the antibacterial mechanism of CuO nanoparticles: revealing the route of induced oxidative stress. *Small*. 2012;8(21):3326-3337.

مستخلص البحث:

يركز هذا البحث على استكشاف الإمكانات العلاجية لجسيمات الكبريت النانويه المحضرة من مستخلص *Proteus mirabilis* ضد المكورات العنقودية الذهبية *Staphylococcus aureus* أحد مسببات الأمراض المتورطة في الالتهابات الجلدية. حددت الدراسة تأثيرات مثبطة كبيرة لهذه الجسيمات النانوية على عزلات المكورات العنقودية الذهبية المنتجة للأغشية الحيوية والمقاومة للأدوية المتعددة (A5، A8، A9، A11، وA29)، مع تركيزات مثبطة دنيا تتراوح بين 16 إلى 32 ميكروغرام/مل. في حين لم تجد الدراسة فروق ذات دلالة إحصائية في معدلات التثبيط عبر تركيزات الجسيمات النانوية المختلفة ($P = 0.842$)، كانت هناك زيادة ملحوظة في النشاط المضاد للأغشية الحيوية بتركيزات أعلى ($p<0.05$). على سبيل المثال، عند 1024 ميكروغرام/مل، كان معدل التثبيط حوالي 93.1%، مقارنة بـ 5.2% عند 2 ميكروغرام/مل ($p=0.0001$). تؤكد هذه النتائج على الفعالية المضادة للميكروبات الواعدة للجسيمات النانوية الكبريتية المشتقة من *Proteus mirabilis* في مكافحة عدوى المكورات العنقودية الذهبية المقاومة للأدوية والمكونه للأغشيه الحيويه والمرتبطة عادة بالتهاب الجلد.